



Article scientifique

Article

2022

Accepted version

Open Access

This is an author manuscript post-peer-reviewing (accepted version) of the original publication. The layout of the published version may differ .

---

## Inhibition of IL-1 $\beta$ release from macrophages targeted with necrosulfonamide-loaded porous nanoparticles

---

Boersma, Bart Nicolaas; Möller, Karin; Wehl, Lisa; Puddinu, Viola; Huard, Arnaud; Fauteux-Daniel, Sébastien; Bourquin, Carole; Palmer-Lourenco, Gaby; Bein, Thomas

### How to cite

BOERSMA, Bart Nicolaas et al. Inhibition of IL-1 $\beta$  release from macrophages targeted with necrosulfonamide-loaded porous nanoparticles. In: Journal of controlled release, 2022, vol. 351, p. 989–1002. doi: 10.1016/j.jconrel.2022.09.063

This publication URL: <https://archive-ouverte.unige.ch/unige:164425>

Publication DOI: [10.1016/j.jconrel.2022.09.063](https://doi.org/10.1016/j.jconrel.2022.09.063)

# Journal of Controlled Release

## Inhibition of IL-1 $\beta$ Release from Macrophages with Necrosulfonamide-Loaded Porous Nanoparticles --Manuscript Draft--

<b>Manuscript Number:</b>	COREL-D-22-01606R1
<b>Article Type:</b>	VSI: ESCDD2022
<b>Keywords:</b>	Drug Delivery; mesoporous nanoparticles; mesoporous silica nanoparticles (MSN); cyclodextrin nanoparticles; necrosulfonamide; pyroptosis; gasdermin D; IL-1 $\beta$ ; Macrophages; Inflammation
<b>Corresponding Author:</b>	Karin Möller, PhD Ludwig Maximilians University Munich München, GERMANY
<b>First Author:</b>	Karin Möller, PhD
<b>Order of Authors:</b>	Karin Möller, PhD Bart Boersma Lisa Wehl Viola Puddinu Arnaud Huard, PhD Sébastien Fauteux-Daniel, PhD Carole Bourquin, Prof Gaby Palmer, Prof Thomas Bein, Prof
<b>Abstract:</b>	<p>Inflammation is required for protective responses against pathogens and is thus essential for survival, but sustained inflammation can lead to diseases, such as atherosclerosis and cancer. Two important mediators of inflammation are the cytokines IL-1<math>\beta</math> and IL-18, which are produced by myeloid cells of the immune system, including macrophages. These cytokines are released into the extracellular space through pores formed in the plasma membrane by the oligomerized protein gasdermin D (GSDMD). Necrosulfonamide (NSA) was recently identified as an effective GSDMD inhibitor and represents a promising therapeutic agent in GSDMD-dependent inflammatory diseases. Here, we targeted NSA to both mouse and human macrophages by using three different types of porous nanoparticles (NP), i.e. mesoporous silica (MSN), porous crosslinked cyclodextrin carriers (CD-NP), and a mesoporous magnesium-phosphate carrier (MPC-NP), all displaying high loading capacities for this hydrophobic drug. Cellular uptake and intracellular NSA delivery were tracked in time-lapse experiments by live-cell, high-throughput fluorescence microscopy, demonstrating rapid nanoparticle uptake and effective targeted delivery of NSA to phagocytic cells. Notably, a strong cytostatic effect was observed when a macrophage cell line was exposed to free NSA. In contrast, cell growth was much less affected when NSA was delivered via the nanoparticle carriers. Utilizing NSA-loaded nanoparticles, a successful concentration-dependent suppression of IL-1<math>\beta</math> secretion from freshly differentiated primary murine and human macrophages was observed. Functional assays showed the strongest suppressive effect on human macrophages when using CD-NP for NSA delivery, followed by MSN-NP. In contrast, MPC-NP completely blocked the metabolic activity in macrophages when loaded with NSA. This study demonstrates the potential of porous nanoparticles for the effective delivery of hydrophobic drugs to macrophages in order to suppress inflammatory responses.</p>

To Prof. Jos Paulusse  
JCR Special Issue Editor  
Department of Biomolecular Nanotechnology  
University of Twente  
Enschede, The Netherlands

Munich, September 26, 2022

Dear Jos,

We are happy to submit the revised manuscript.

Enclosed please find now our revised manuscript entitled:

**Inhibition of IL-1 $\beta$  Release from Macrophages Targeted with  
Necrosulfonamide-Loaded Porous Nanoparticles**

by Bart Boersma, Karin Möller\*, Lisa Wehl, Viola Puddinu, Arnaud Huard, Sébastien Fauteux-  
Daniel, Carole Bourquin, Gaby Palmer, Thomas Bein

Dr. Karin Möller  
Department of Chemistry  
Ludwig-Maximilians-Universität München (LMU)  
Butenandtstr. 5-13 (E)  
81377 München  
Germany  
Tel.: +49-89-2180-77621  
Fax: +49-89-2180-77622  
K.Moeller@lmu.de

## **Response to reviewers**

We thank the reviewers for their positive assessment and their constructive suggestions. We have addressed all comments and suggestions and have changed the original manuscript accordingly as specified below. All changes are indicated in yellow highlightings.

### **Reviewer #1:**

#### **1. Ethical approval number for the animals studies should be added.**

A1. We have now added the animal approval number in the supplement to the paragraph « Generation of murine bone marrow-derived macrophages (BMDM) ».

#### **2. Mesoporous silica and crosslinked cyclodextrin nanocarriers performed better than mesoporous magnesium-phosphate carriers and it is suggested to include this information in the abstract.**

A2. To include this information, we have added the following sentence to the abstract :

« Functional assays showed the strongest suppressive effect on human macrophages when using CD-NP for NSA delivery, followed by MSN-NP. In contrast, MPC-NP completely blocked the metabolic activity in macrophages when loaded with NSA. »

### **Reviewer #2:**

#### **1. The payload was absorbed in the pores of the nanoparticles by physical means, but how was NSA released and how can the release be controlled? Was it due to degradation of the nanoparticles or simply diffusion of the compound?**

A1. As we have documented in the SI, we did not measure a substantial release of NSA from the nanoparticles into aqueous media under various conditions, even in absence of a nanoparticle-encapsulating DOTAP/DOPC bilayer. The timescale of nanoparticle degradation, while different for the different particle types, is far slower than the appearance of NSA fluorescence in the cells, which occurs within minutes after exposure of the cells. We thus propose that the release of NSA from the pores of the nanoparticles is driven by the NSA concentration gradients between nanoparticle interior and lipophilic components in the cells such as membranes and compartments. We have included the following sentence in the manuscript (p.11):

« In summary, NSA delivery into cells occurs on a similar time scale with free NSA as well as through NP delivery. Since a premature release of NSA from MSN-NP into aqueous phases was not observed as described above, and having established a very rapid phagocytosis/membrane attachment of the nanoparticles, we propose that the intracellular NSA release from the nanoparticles occurs via diffusion along concentration gradients, driven by the lipophilic character of NSA upon contact with lipophilic intracellular components. »

#### **2. How did DD reduce the uptake of the particles in DC, macrophages and B cells? This should be discussed. DD contains cationic components and this should theoretically enhance cellular uptake of nanoparticles.**

A2. There is indeed an abundant literature showing that uptake by myeloid cells and B cells can be increased for cationic particles. However, other studies have shown that in some cases, cationic particles may affect the physiology of the phagocytic cell, rather than the uptake. In particular, cationic particles can modulate the activation and the metabolism of the cells. Thus, the uptake may depend not only on the surface charge, but also on the precise composition of the coating, as well as the size and shape of the particles.

We have added the following sentence and a literature reference into the discussion:

« This effect may be traced to a bilayer-induced modulation of the metabolism in the phagocytic cells.[1] »

**3. One important point to be clarified is the rationale of formulating NSA in nanoparticles? In the current study, the experiments were all performed *in vitro* and the high benefit of nanoformulation of NSA is not demonstrated.**

A3. The rationale for formulating NSA in nanoparticles is first to target the drug to macrophages and other phagocytic cells. This drug has demonstrated toxicity towards other immune cells, [2] so that nanoparticle targeting could at the same time enhance the effect of NSA on macrophages and decrease the off-target toxicity of DMSO-derived NSA. Indeed, we have shown here that nanoparticles are effective for targeting, as NSA-NP were better taken up by phagocytic cells than by non-phagocytic cells. Most importantly, we have shown in this work that NSA-NP were better tolerated by macrophages than the free NSA compound.

Although this study focused on the characterization of NSA-NP and on their *in vitro* effects on macrophages and other immune cells, we expect additional benefits of the nanoparticle formulation *in vivo*. Indeed, we have previously shown that following subcutaneous injection, MSN nanoparticles accumulate in phagocytic cells in the lymph nodes draining the injection site.[3] Nanoparticle formulation may therefore allow site-specific delivery of NSA. Furthermore, encapsulating NSA in nanoparticles avoids the exposure to DMSO, which is otherwise required for this highly insoluble drug when employing a carrier-free delivery. The *in vivo* benefits of nanoparticle delivery of NSA will be investigated in future studies.

We feel that we have addressed the general potential of NP delivery in the introduction of this manuscript, reading as follows:

« the extremely hydrophobic nature of this molecule complicates drug administration *in vivo* since it requires the use of potentially toxic organic solvents. Furthermore, NSA has demonstrated toxicity towards immune cells and, as a small molecule, may present less than ideal pharmacokinetic behavior within the organism.

To overcome limitations with respect to limited stability, unfavorable pharmacokinetics and the potential toxicity of small (hydrophobic) molecular delivery, different nano-carrier systems have been developed over the years... “

Concerning the potential of these NP for *in vivo* applications, we have added the following sentence in the outlook of this manuscript:

“Here, we have focused on the characterization of different NSA-NP systems and on their *in vitro* effects on macrophages and other immune cells. However, we expect additional benefits of these nanoparticle formulations *in vivo*. Indeed, we have previously shown that following subcutaneous injection, MSN nanoparticles accumulate in phagocytic cells in the lymph nodes draining the injection site.[3] Nanoparticle formulation may therefore also allow for site-specific, DMSO-free delivery of NSA *in vivo*. “

\*\*\*

Summarizing, we believe that we have addressed all questions and comments noted by the reviewers and we thank the reviewers again for their thoughtful evaluation of our manuscript.

We hope that the manuscript is now suitable for publication.

- [1] A.K. Dey, A. Nougarede, F. Clément, C. Fournier, E. Jouvin-Marche, M. Escudé, D. Jary, F.P. Navarro, P.N. Marche, Tuning the Immunostimulation Properties of Cationic Lipid Nanocarriers for Nucleic Acid Delivery, *Frontiers in Immunology*, 12 (2021), Article 722411.
- [2] X. Chen, W.-t. He, L. Hu, J. Li, Y. Fang, X. Wang, X. Xu, Z. Wang, K. Huang, J. Han, Pyroptosis is driven by non-selective gasdermin-D pore and its morphology is different from MLKL channel-mediated necroptosis, *Cell Research*, 26 (2016) 1007-1020.
- [3] J. Wagner, D. Gößl, N. Ustyanovska, M. Xiong, D. Hauser, O. Zhuzhgova, S. Hočevar, B. Taskoparan, L. Poller, S. Datz, H. Engelke, Y. Daali, T. Bein, C. Bourquin, Mesoporous Silica Nanoparticles as pH-Responsive Carrier for the Immune-Activating Drug Resiquimod Enhance the Local Immune Response in Mice, *ACS Nano*, 15 (2021) 4450-4466.

# Inhibition of IL-1 $\beta$ Release from Macrophages Targeted with Necrosulfonamide-Loaded Porous Nanoparticles

Bart Boersma<sup>a,b,1</sup>, Karin Möller<sup>c,1,\*</sup>, Lisa Wehl<sup>c,1</sup>, Viola Puddinu<sup>a</sup>, Arnaud Huard<sup>d,e</sup>, Sébastien Fauteux-Daniel<sup>d,e</sup>, Carole Bourquin<sup>a,f,2</sup>, Gaby Palmer<sup>d,e,2</sup>, Thomas Bein<sup>c,2</sup>

a Institute of Pharmaceutical Sciences of Western Switzerland, University of Geneva, 1211 Geneva, Switzerland;

b School of Pharmaceutical Sciences, University of Geneva, 1211 Geneva, Switzerland.

c Department of Chemistry and Center for NanoScience (CeNS), Ludwig-Maximilians-Universität München (LMU), Germany

d Department of Medicine, Faculty of Medicine, University of Geneva, 1211 Geneva, Switzerland

e Department of Pathology and Immunology, Faculty of Medicine, University of Geneva, 1211 Geneva, Switzerland

f Department of Anesthesiology, Pharmacology and Intensive Care, Faculty of Medicine, University of Geneva, 1211 Geneva, Switzerland.

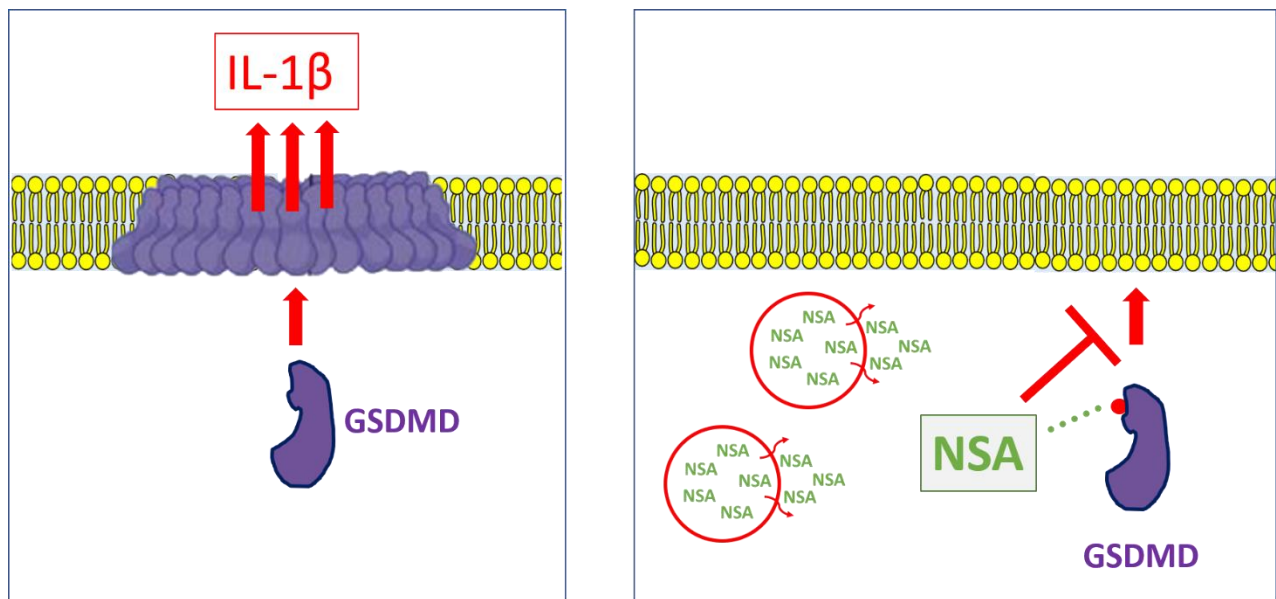
<sup>1,2</sup> These authors contributed equally to this work

\* Corresponding author:

K. Möller [K.Moeller@lmu.de](mailto:K.Moeller@lmu.de)

**Keywords:** drug delivery, mesoporous nanoparticles, mesoporous silica nanoparticles (MSN), cyclodextrin nanoparticles, necrosulfonamide, pyroptosis, gasdermin D, IL-1 $\beta$ , macrophages, inflammation

## Graphical abstract



Activated gasdermin D (GSDMD) polymerizes to form transmembrane pores, which allow release of pro-inflammatory mediators, such as IL-1 $\beta$ , and lead to cell death by pyroptosis. The recently discovered necrosulfonamide (NSA) binds to GSDMD, inhibiting pore formation. This hydrophobic agent was successfully delivered via different porous nanoparticles to murine and human macrophages and suppressed the release of IL-1 $\beta$  in a concentration-dependent manner.



# Inhibition of IL-1 $\beta$ Release from Macrophages Targeted with Necrosulfonamide-Loaded Porous Nanoparticles

Bart Boersma<sup>a,b,1</sup>, Karin Möller<sup>c,1,\*</sup>, Lisa Wehl<sup>c,1</sup>, Viola Puddinu<sup>a</sup>, Arnaud Huard<sup>d,e</sup>, Sébastien Fauteux-Daniel<sup>d,e</sup>, Carole Bourquin<sup>a,f,2</sup>, Gaby Palmer<sup>d,e,2</sup>, Thomas Bein<sup>c,2</sup>

a Institute of Pharmaceutical Sciences of Western Switzerland, University of Geneva, 1211 Geneva, Switzerland;

b School of Pharmaceutical Sciences, University of Geneva, 1211 Geneva, Switzerland.

c Department of Chemistry and Center for NanoScience (CeNS), Ludwig-Maximilians-Universität München (LMU), Germany

d Department of Medicine, Faculty of Medicine, University of Geneva, 1211 Geneva, Switzerland

e Department of Pathology and Immunology, Faculty of Medicine, University of Geneva, 1211 Geneva, Switzerland

f Department of Anesthesiology, Pharmacology and Intensive Care, Faculty of Medicine, University of Geneva, 1211 Geneva, Switzerland.

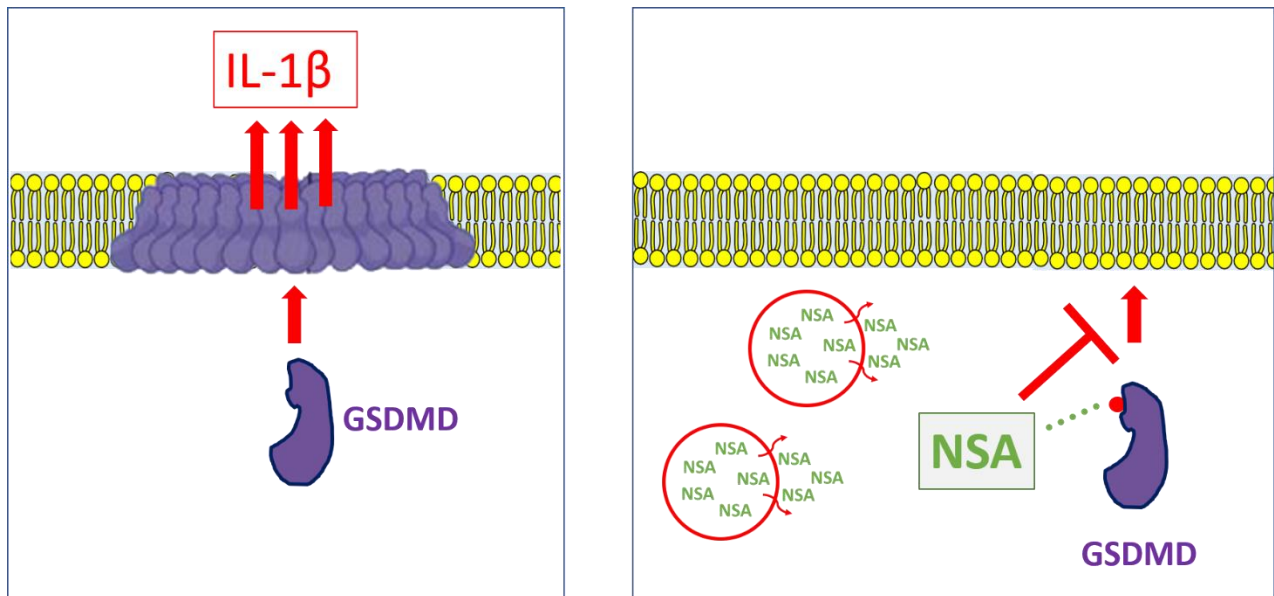
<sup>1,2</sup> These authors contributed equally to this work

\* Corresponding author:

K. Möller [K.Moeller@lmu.de](mailto:K.Moeller@lmu.de)

**Keywords:** drug delivery, mesoporous nanoparticles, mesoporous silica nanoparticles (MSN), cyclodextrin nanoparticles, necrosulfonamide, pyroptosis, gasdermin D, IL-1 $\beta$ , macrophages, inflammation

## Graphical abstract



Activated gasdermin D (GSDMD) polymerizes to form transmembrane pores, which allow release of pro-inflammatory mediators, such as IL-1 $\beta$ , and lead to cell death by pyroptosis. The recently discovered necrosulfonamide (NSA) binds to GSDMD, inhibiting pore formation. This hydrophobic agent was successfully delivered via different porous nanoparticles to murine and human macrophages and suppressed the release of IL-1 $\beta$  in a concentration-dependent manner.

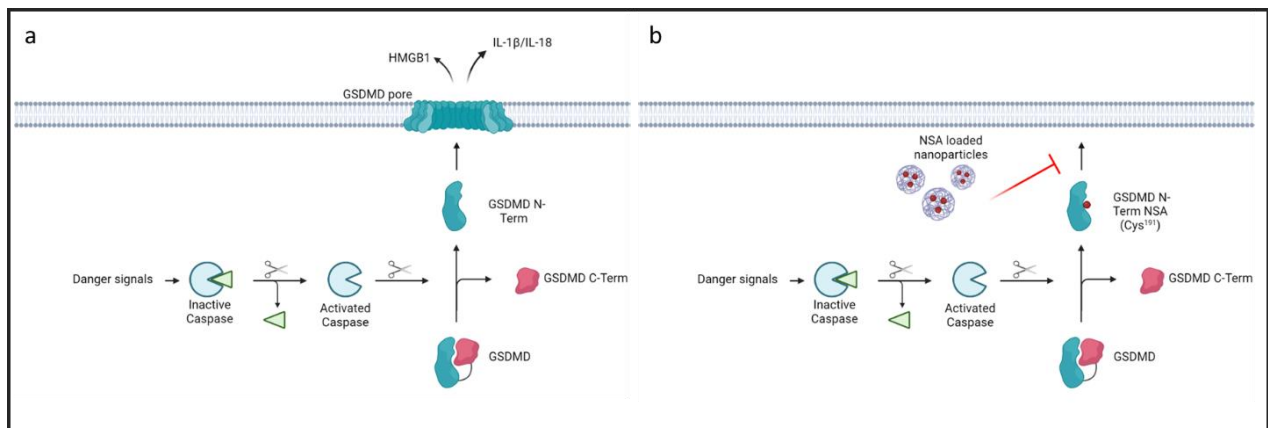
## Abstract

Inflammation is required for protective responses against pathogens and is thus essential for survival, but sustained inflammation can lead to diseases, such as atherosclerosis and cancer. Two important mediators of inflammation are the cytokines IL-1 $\beta$  and IL-18, which are produced by myeloid cells of the immune system, including macrophages. These cytokines are released into the extracellular space through pores formed in the plasma membrane by the oligomerized protein gasdermin D (GSDMD). Necrosulfonamide (NSA) was recently identified as an effective GSDMD inhibitor and represents a promising therapeutic agent in GSDMD-dependent inflammatory diseases. Here, we targeted NSA to both mouse and human macrophages by using three different types of porous nanoparticles (NP), i.e. mesoporous silica (MSN), porous crosslinked cyclodextrin carriers (CD-NP), and a mesoporous magnesium-phosphate carrier (MPC-NP), all displaying high loading capacities for this hydrophobic drug. Cellular uptake and intracellular NSA delivery were tracked in time-lapse experiments by live-cell, high-throughput fluorescence microscopy, demonstrating rapid nanoparticle uptake and effective targeted delivery of NSA to phagocytic cells. Notably, a strong cytostatic effect was observed when a macrophage cell line was exposed to free NSA. In contrast, cell growth was much less affected when NSA was delivered via the nanoparticle carriers. Utilizing NSA-loaded nanoparticles, a successful concentration-dependent suppression of IL-1 $\beta$  secretion from freshly differentiated primary murine and human macrophages was observed. Functional assays showed the strongest suppressive effect on human macrophages when using CD-NP for NSA delivery, followed by MSN-NP. In contrast, MPC-NP completely blocked the metabolic activity in macrophages when loaded with NSA. This study demonstrates the potential of porous nanoparticles for the effective delivery of hydrophobic drugs to macrophages in order to suppress inflammatory responses.

# Introduction

Inflammation is a physiological response of the organism that is essential for the defense against pathogens. However, chronic inflammation can be detrimental for many diseases, including cardiovascular and autoimmune disorders, as well as different types of cancer.[1, 2] Two major mediators of inflammation are the cytokines interleukin (IL)-1 $\beta$  and IL-18, which are released from immune cells, such as macrophages, upon activation by danger signals from pathogens or by endogenous stress signals. The release of these cytokines can trigger and sustain inflammatory processes throughout the body.[1, 3]

The release of IL-1 $\beta$  and IL-18 from immune cells is the result of a sequential process illustrated in Scheme 1a. First, the detection by sensor proteins of bacterial or viral components, which function as danger signals, triggers a cascade of intracellular events leading to the activation of caspase-1 by proteolytic cleavage. Activated caspase-1 is in turn able to cleave several other proteins, including the proforms of IL-1 $\beta$  and IL-18 and the pore-forming protein gasdermin D (GSDMD).[4, 5] GSDMD cleavage liberates its N-terminal domain, which oligomerizes to form a 10–14 nm pore that inserts into the plasma membrane.[6, 7] Ultimately, GSDMD-mediated pore formation allows the release of pro-inflammatory mediators, such as IL-1 $\beta$ , IL-18, high mobility group box 1 (HMGB1) and adenosine triphosphate (ATP) and results in a form of inflammatory cell death termed pyroptosis.[8]



Scheme 1. Schematic overview of the GSDMD activation mechanism resulting in transmembrane pore formation and cytokine release (a) and its blocking through particle-delivered NSA (b).

Recently, high-throughput screening efforts have identified two GSDMD pore formation antagonist molecules, disulfiram and necrosulfonamide (NSA); see Fig. 2 for the structure of NSA.[9-11] NSA inhibits GSDMD pore formation by binding directly to Cys191 of human GSDMD or to Cys192 of mouse GSDMD.[10] By preventing pore formation, NSA inhibits the release of pro-inflammatory mediators such as IL-1 $\beta$  (Scheme 1b). NSA thus represents a promising new

effector molecule against GSDMD-dependent inflammation. However, the extremely hydrophobic nature of this molecule complicates drug administration *in vivo* since it requires the use of potentially toxic organic solvents. Furthermore, NSA has demonstrated toxicity towards immune cells and, as a small molecule, may present less than ideal pharmacokinetic behavior within the organism.[12]

To overcome limitations with respect to limited stability, unfavorable pharmacokinetics and the potential toxicity of small (hydrophobic) molecular delivery, different nano-carrier systems have been developed over the years.[13] These are made of organic materials such as polymers, micelles and liposomes or consist of solid/porous inorganic materials. Especially porous nanocarriers have evolved as promising drug-carrier systems because they allow for an internal encapsulation of small molecular drugs within the host as opposed to an attachment onto the surface of solid nanoparticles (NP). In this way, toxicity issues or a premature degradation of attached molecules can be avoided. Mesoporous silica NP are a prominent class of porous carrier systems, which have proven to be effective delivery agents for a broad range of applications, including cancer (immuno)-therapy, combination drug delivery or gene delivery.[14-20] Similarly, cyclodextrins[21] and crosslinked cyclodextrin-based NP [22, 23] show a high capacity to encapsulate both hydrophobic and hydrophilic drugs and were found to improve the solubility of poorly water-soluble molecules.[24]

In this work, we explore for the first time the feasibility of targeting NSA to macrophages with porous NP. In addition to their ability to initiate inflammation, an essential function of macrophages is their capacity to engulf particulate material such as bacteria or dying cells by phagocytosis.[25] We have taken advantage of this specialized function by using NP as vehicle to deliver NSA specifically to macrophages and other phagocytic cells. We show that the exposure of murine and human macrophages to these NSA-loaded carriers enables a solvent-free NSA delivery that inhibits release of proinflammatory IL-1 $\beta$ . Three in-house developed nanocarriers featuring different composition and structure were evaluated in this study. The nanocarriers comprise mesoporous silica nanoparticles (MSN), our newly developed covalently crosslinked cyclodextrin NP (CD-NP) and recently established mesoporous magnesium phosphate NP (MPC).[26] The efficacy of NP cellular uptake, NSA delivery and toxicity were studied using a macrophage cell line and primary mouse splenocytes. Murine bone marrow-derived macrophages (BMDM), as well as human monocyte-derived macrophages (MDM) were then used to evaluate the efficacy of cytokine suppression upon NSA delivery. Overall, we demonstrate that a high NSA loading capacity is reached with our nanocarrier systems and that NSA delivery is successful and efficient with several of the carriers, as established by a concentration-dependent suppression of the GSDMD-mediated release of IL-1 $\beta$ . Importantly, the toxicity of NSA towards immune cells is strongly reduced by NP delivery.

# Results

## Synthesis and characterization of nanoparticles

Three different materials were evaluated for their ability to efficiently deliver NSA to immune cells. All porous nanocarriers used in this project are biocompatible and were chosen for their beneficial properties regarding a sustained, solvent-free drug delivery. The robust NP stability often allows for a storage in ethanolic solutions for years and thus potential “off-the-shelf” applications. Nevertheless, such NP are completely degradable under drug-delivery conditions, as established, for example, for mesoporous silica NP (MSN).[27, 28] Their large surface areas and the presence of mesopores are suitable for the uptake of large amounts of NSA into their internal cavities. All NP used here were synthesized with or without a lipid bilayer consisting of a cationic dioleoyl-containing lipid mixture (DOTAP/DOPC, DD). This was done for two reasons: a) to study its impact on cell uptake, and b) to provide a shield against premature drug release.

The first class of materials used in this study, MSN, has been continuously developed in our group over the years and was used in diverse biomedical applications based on their exceptional flexibility with respect to particle and pore size, as well as NP composition and molecular functionalization.[29, 30] For the adsorption of the hydrophobic molecule NSA, we synthesized core-shell MSN consisting of a silica core functionalized with 5 wt% of a phenylsilane precursor in order to create a hydrophobic interior. The outer MSN surface was then co-condensed with 2 wt% mercaptopropyl-triethoxysilane to create a negatively charged particle surface decorated with mercapto-groups for future fluorophore attachment or bilayer adhesion. These particles have an average size of about 80 nm based on transmission electron microscopy (TEM) (see Fig. 1a, b) and a hydrodynamic particle size of around 245 nm in water as measured by dynamic light scattering (DLS; see SI Table 1). A large surface area of 1098 m<sup>2</sup>/g was determined with nitrogen sorption. A relatively small pore size of 3.4 nm with a pore volume of 0.75 cm<sup>3</sup>/g was implemented here to best fit the dimensions and diffusive transport of the small NSA guest molecules (Fig. 1c, d).

The second class of materials consists of new cyclodextrin-based nanoparticles (CD-NP). Cyclodextrin-based materials have been used as carriers for anti-inflammatory drugs before.[31] Pioneering work creating crosslinked cyclodextrin ‘nanosponge’ materials was performed by the group of Trotta, who used carbonyl- or dicarboxylate-based linker molecules.[32, 33] Here, we synthesized nanoparticles of cyclodextrin by covalently cross-linking  $\alpha$ -cyclodextrin with carbonyldiimidazole (CDI) in dimethylformamide (DMF). These particles were subsequently stabilized by addition of polyethylene glycol (PEG). The NP were finally precipitated with water, resulting in NP with a controlled particle size distribution and a hydrodynamic diameter of around 195 nm in water (DLS). The dried powder shows a particle size of 90 nm in the scanning electron microscope (SEM; Fig. 1e, f). Cyclodextrin NP are promising materials because they offer small integrated cavities of 0.7 nm with hydrophobic character originating from the  $\beta$ -CD molecular subunits. By crosslinking these units with spacer molecules such as

tetrafluoroterephthalonitrile (TFTN) or CDI, nanoparticles with added interstitial adsorption sites are generated.[34] This creates space for additional guest adsorption, thus expanding the molecular capacity of the CD entities as recently demonstrated with related  $\beta$ -CD-TFTN NP for the adsorption of hydrophobic curcumin.[35] The high adsorption capacity of CD-CDI NP becomes apparent upon NSA loading (please consult the Supplemental Information (SI) for further details of materials synthesis and characterisation). We have also evaluated NSA delivery with the mentioned TFTN crosslinked CD-NP (CD-TFTN-NP). Although NSA delivery was successful with this carrier system, cellular toxicity was observed already in the unloaded state (data not shown). We therefore concentrated our efforts on the alternative cyclodextrin NP crosslinked via CDI - linker (CD-NP).

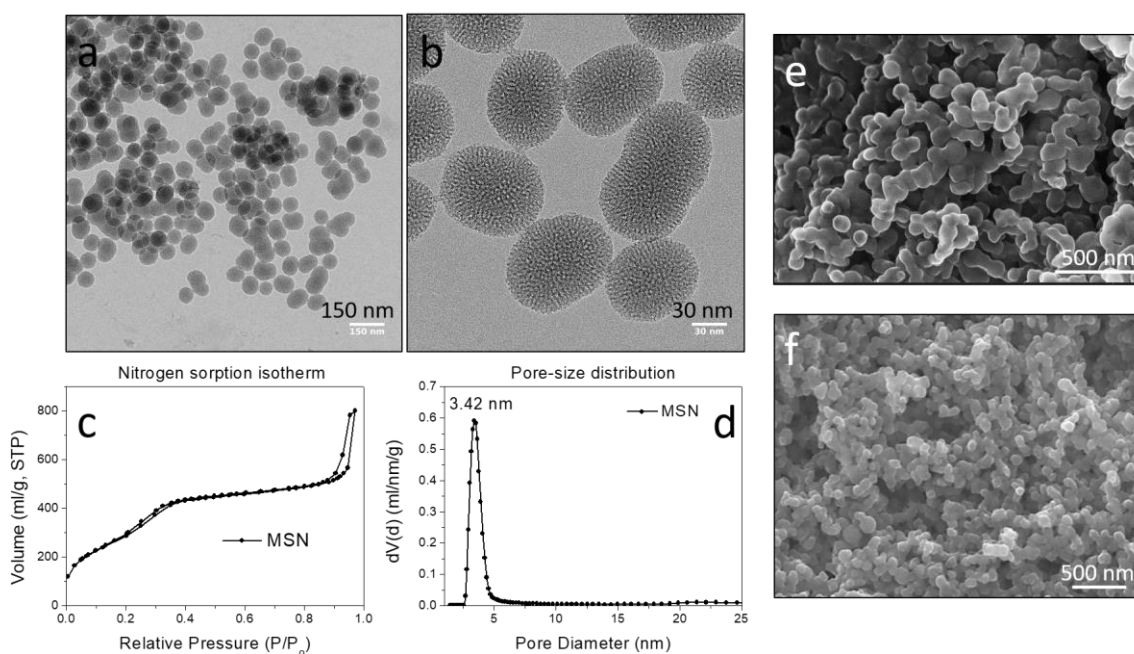


Fig. 1. MSN, CD- and MPC-NP materials characterization. a,b) TEM images of MSN, c,d) MSN nitrogen sorption isotherm and pore size distribution. e) SEM images of CD-CDI-NP, f) SEM images of MPC-NP.

The third material is composed of completely biogenic magnesium phosphate citrate NP (MPC-NP). We recently showed that a cetyltrimethylammonium (CTAC)-templated precipitation method resulted in evenly sized MPC NP of around 80 nm diameter (SEM).[36] Nitrogen sorption established a high surface area of 560 m<sup>2</sup>/g of template-extracted particles and most importantly, a high pore volume of 0.8 cm<sup>3</sup>/g originating from pores of 6.3 nm. These particles are stable at neutral to basic conditions when coated with a DOTAP/DOPC lipid bilayer, however, are completely biodegradable under acidic conditions at pH 5.5.

In the following, we will describe cellular interactions with MSN carriers in more detail and refer to the other carrier systems where applicable.

## Porous NP show high loading capacities for NSA

The uptake of NSA into the pores of the different carriers is conveniently followed by UV-VIS spectroscopy. NSA displays a prominent absorption band at 377 nm (see SI, Fig. S1) that allows one to determine the uptake by difference calculation regarding the NSA amounts offered in solution. Loading efficiencies (amount taken up vs. amount offered) calculated after extensive washings were usually high for all materials, ranging from 80 to 95%. When a standard amount of 200  $\mu\text{g}$  NSA was offered to 1 mg of carrier, an uptake between 16-19 wt% was reached. Samples with this loading level were used for all cell experiments for comparability. In principle, however, it is possible to increase the loading capacity up to 49 wt% in MSN, up to 29% in CD-NP or up to 32 wt% in MPC-NP.

The rapid and nearly complete absorption of NSA into the MSN carrier was indicated when the light-yellow suspension of MSN and added NSA was centrifuged. A yellow cake and a nearly clear supernatant were obtained (see SI, Fig. S2). UV-Vis analysis confirmed that most of the NSA had been adsorbed, even after a short exposure time of 30 minutes. Spectroscopic evidence of the NSA uptake was further obtained with FT-Raman spectroscopy (Fig. 2). In contrast to FTIR spectroscopy that showed only very weak additional signals of NSA in the MSN NP, prominent Raman signals were obtained due to the phenyl, thiophene, pyrazine as well as the sulfoxide groups present in NSA (purple trace in Fig. 2). While MSN particles (blue) show weak Raman scattering, strong peaks were observed from NSA in MSN. In addition, NSA-MSN show significant shifts in position as well as relative intensity with respect to the solid NSA precursor, pointing to strong interactions with the internal MSN surface.

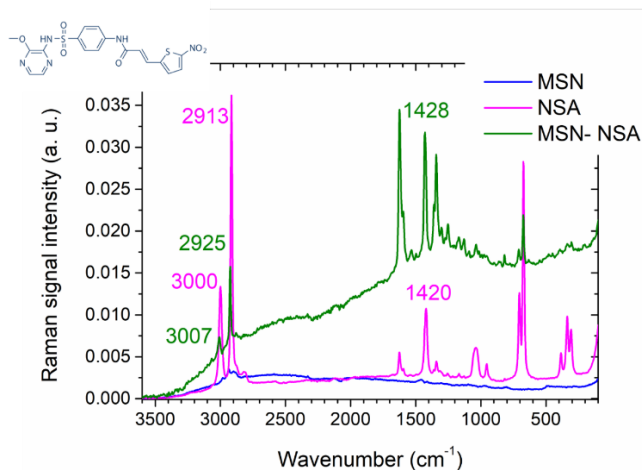


Fig. 2: FT-Raman spectroscopy of the carrier MSN (blue), NSA powder (purple) and NSA absorbed in MSN (green).

The apparent dimensions (hydrodynamic diameter) of the NP when measured in solution are dependent on the dispersing agent and are least influenced in an ethanolic solution. For instance,



for unloaded MSN, we observe a particle size of 140 nm in ethanolic solution that increases to 245 nm in aqueous solution. CD-NP have a particle size of 195 nm in water, yet the measured particle size of dry CD-NP is 90 nm as obtained by SEM. However, even after loading with NSA, the application of a lipid bilayer (coded DD = DOTAP/DOPC), or after addition of a fluorophore for imaging, hydrodynamic diameters were all around 200 nm or below (see Fig.3 as well as SI Fig. S3 and Table 1). These dimensions are suitable for cell experiments, where NP samples with and without a lipid bilayer were used to study their cellular uptake.

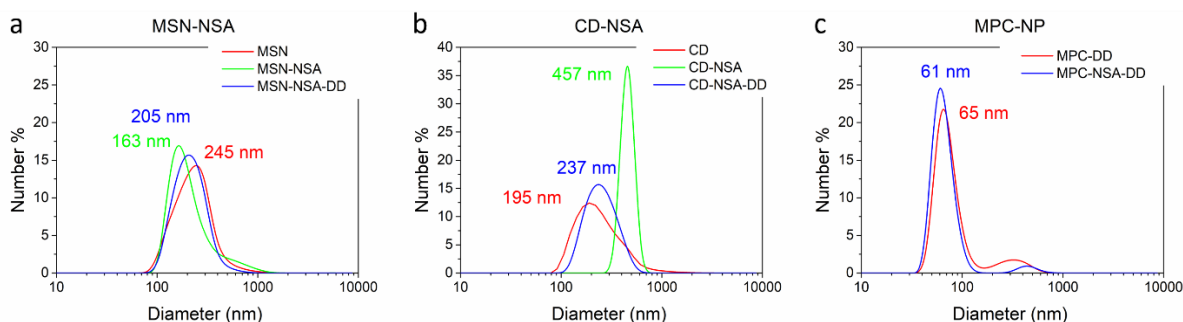


Fig. 3: Dynamic light scattering (DLS) curves of NSA-loaded samples in water with and without a lipid bilayer (DD), a) MSN, b) CD and c) MPC NP.

Following the absorption of NSA, MSN samples with or without a lipid bilayer were examined regarding spontaneous NSA release in different media. No release was measurable by UV-Vis spectroscopy when samples were dispersed in aqueous solution and stirred for 1 h at pH 7 or pH 5. Even in cell medium (fluobrite DMEM) or medium containing 10% of fetal bovine serum (FBS) the release was minimal with or without a lipid bilayer, ranging between 2-5% of the absorbed NSA (see SI, Fig. S4). We can therefore assume that no significant premature release would occur in cell experiments with these NP even without a lipid bilayer.

### Rapid phagocytosis of NSA-loaded nanoparticles and fast release of NSA in a murine macrophage cell line

First, we examined the rate of uptake of unloaded MSN-NP in the murine macrophage cell line RAW 264.7. In order to follow the uptake by fluorescence microscopy, we labeled the particles with a red fluorophore resulting in MSN-633 NP. RAW 264.7 cells seeded in a 96-well plate were placed into an environmental chamber located directly within the microscope. Cells were kept at 37 °C and 5% CO<sub>2</sub> atmosphere to perform time-lapse measurements every 3 minutes over 3 h. Images were obtained at a 40x magnification. Selected time intervals are shown in Figure 4

(transmitted light and red fluorescence channel). The first image was collected as soon as possible after NP addition, after about 3 minutes. Strikingly, MSN particles were almost immediately associated with cells. NP were clearly seen around the cells, close to the cell wall, directly after sample addition. Accumulation of additional particles within the cells was observed continuously with time, with particles moving deeper into the cellular interior. No particles were observed in the nucleus at any time. No additional particle uptake was observed by visual inspection after about 60 minutes. Following cell division, particles were still detected in daughter cells, albeit at apparently lower amounts per cell, as expected (see SI, Fig S5).

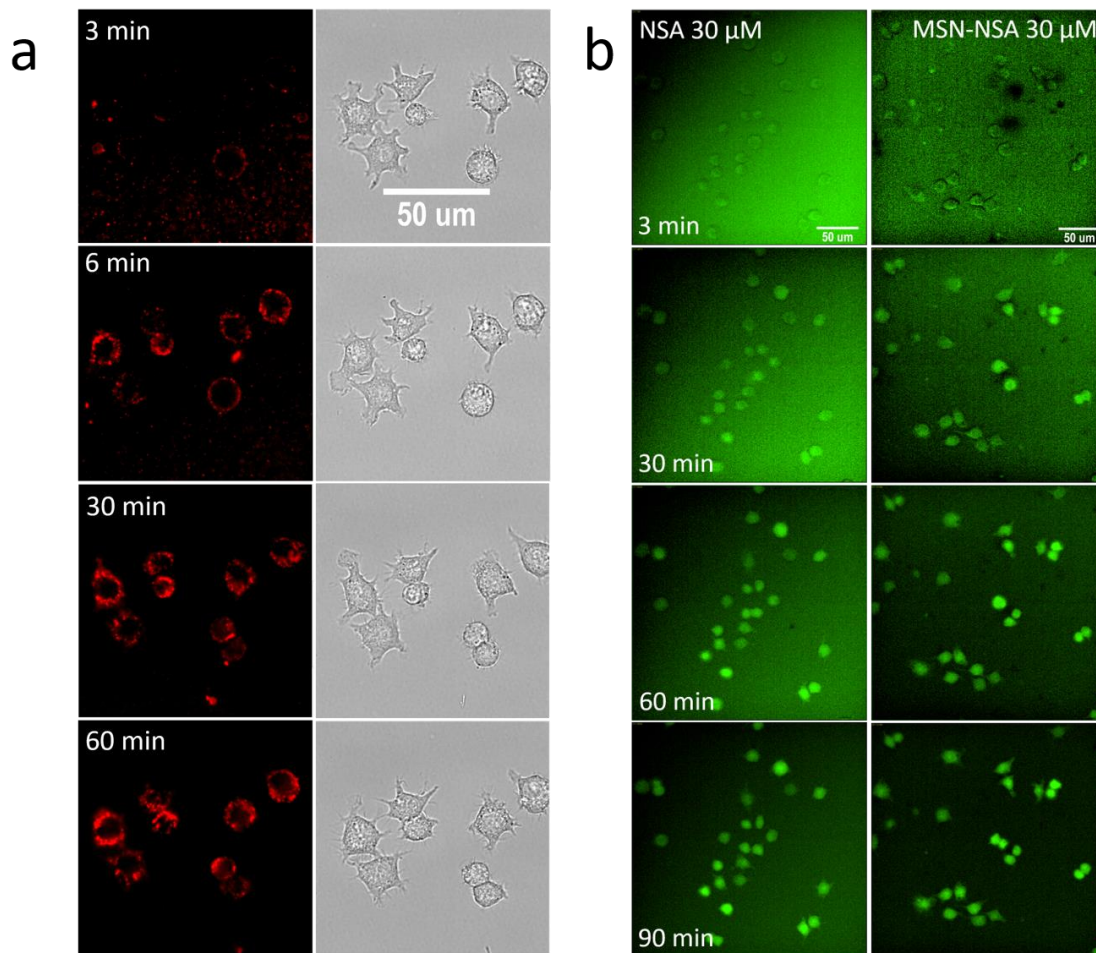


Fig. 4: a) Time-lapse images of RAW 264.7 cells directly after exposure to ATTO-633-labeled MSN (red) NP (40x, transmitted light and CY5 channel). b) Time-lapse images of RAW 264.7 cells directly after exposure to free NSA (left column) or to NSA-loaded MSN-particles of corresponding NSA concentration (right column). NSA was detected in the GFP channel (20x).

Having established a very rapid uptake of the unloaded MSN NP in this macrophage cell line, we examined the rate of NSA delivery by means of MSN carriers. Comparable imaging experiments

were thus performed with either NSA-loaded MSN NP or with free NSA at the same nominal concentrations. As shown in Figure 4b, we observed an increase in green fluorescence originating from the accumulation of NSA in RAW 264.7 cells. Visible evidence of NSA appeared after about 30 minutes and increased in intensity up to about 90 minutes. No major difference in time of uptake was noticed between free NSA and NSA originating from MSN particles. We noticed that NSA started to fluoresce only after accumulating intracellularly. Further, we observed that the NSA was distributed in the cytosol as well as in the nucleus (for higher magnification see SI, Fig. S6).

When the NSA-loaded CD-NP were studied in RAW 264.7 cells, we encountered a comparable time scale of NSA delivery as with MSN particles. While first indications for NSA uptake appeared already after 10 minutes, an evenly distributed green fluorescence in the cytosol was again encountered after 30 minutes. This fluorescence increased in intensity for up to 2 h as seen before. We noticed a difference between MSN and CD NP accumulation in the cells: while MSN NP were readily and strongly taken up by the RAW 264.7 as discussed above, apparently fewer CD NP were encountered within the cells after 2 h incubation. Evidence for NSA delivery with ATTO-633 labeled CD NP, as well as for the cellular uptake as observed with confocal microscopy can be found in the Supplemental information (see SI, Fig. S7). **In summary, NSA delivery into cells occurs on a similar time scale with free NSA as well as through NP delivery. Since a premature release of NSA from MSN-NP into aqueous phases was not observed as described above, and having established a very rapid phagocytosis/membrane attachment of the nanoparticles, we propose that the intracellular NSA release from the nanoparticles occurs via diffusion along concentration gradients, driven by the lipophilic character of NSA upon contact with lipophilic intracellular components.**

#### **Assessment of the toxicity/compatibility of nanoparticles and NSA in a macrophage cell line: unloaded and NSA-loaded nanoparticles are better tolerated than free NSA**

The compatibility of NSA-loaded NP carriers with macrophages was tested on the murine RAW 264.7 macrophage cell line with MSN NP in long-term exposure experiments. Cell growth of the macrophages was monitored using a lensless “Cellwatcher” imaging device. Growth curves of untreated and particle-loaded RAW 264.7 cells were obtained by following the confluency in single wells of a 24-well plate continuously up to about 30 h after NP exposure without medium change. Figure 5a shows a steady increase in confluency of untreated RAW 264.7 cells over time, represented by the black curve. This graph is mirrored by growth curves of cells treated with either unloaded MSN (purple trace) or NSA-loaded MSN, reflecting a 20  $\mu$ M or 30  $\mu$ M NSA concentration (blue and green traces). These results establish that the cells are not compromised in their growth kinetics by the presence of these nanocarriers. Corresponding measurements on RAW 264.7 cells were made with comparable concentrations of free NSA. Here, NSA was added in form of aqueous suspensions derived from a DMSO stock solution. A steady increase of cell proliferation was also observed for these samples, however, displaying slower growth kinetics (Figure 5b). Thus, free NSA inhibits cell proliferation compared to untreated control cells.

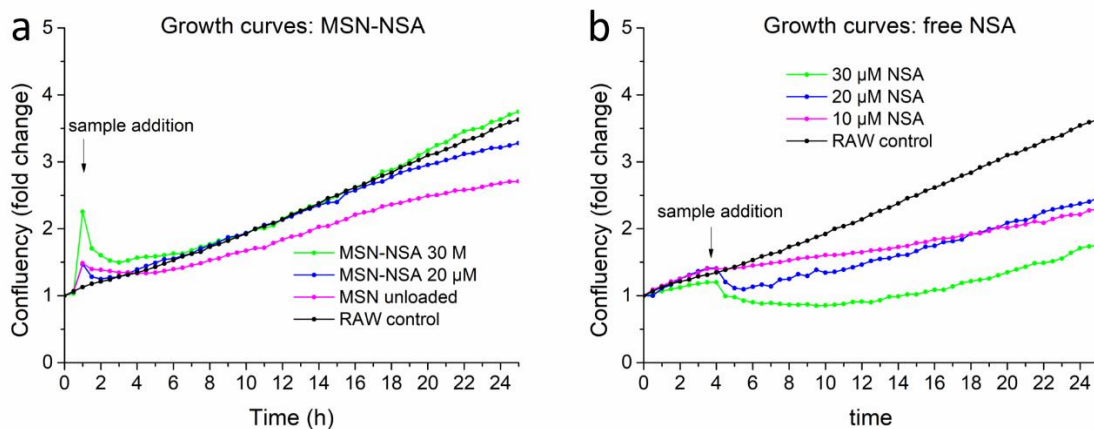


Fig. 5: Compatibility test of RAW 264.7 cells for free NSA and NSA loaded into MSN. Normalized confluency of RAW 264.7 cells in time as measured with a Cellwatcher, a) MSN-exposed cells, growth curves of untreated cells (black trace), cells exposed to unloaded MSN (purple) and MSN-NSA samples (20  $\mu\text{M}$  NSA, blue; 30  $\mu\text{M}$  NSA green. b) free NSA exposed cells, growth curves of untreated cells (black) and cells exposed to increasing concentration of DMSO-derived NSA: 10  $\mu\text{M}$  (purple), 20  $\mu\text{M}$  (blue) and 30  $\mu\text{M}$  (green). Growth curves were normalized to the initial confluency (observed to be around 20%).

Corresponding endpoint images taken after 45 h confirm the greater negative impact of free NSA on cell growth kinetics (see SI, Fig. S8) Notably, all cells were alive at this point and the successful delivery of NSA into the cells was evidenced by the green fluorescence of NSA in all cells (see SI, Fig. S9).

Having established a successful NSA delivery with the NP carrier systems and preserved cell growth following NP exposure, we quantified the metabolic activity of RAW cell response to the unloaded and NSA-loaded carriers. For this we used incubation times of 45 h without performing a medium change.

RAW 264.7 cells were exposed to the different NP, that is, MSN, CD and MPC-NP with increasing concentrations and metabolic activity was measured by an MTT assay. None of the three unloaded carriers showed a substantial impact on metabolic activity up to 100  $\mu\text{g}$  carrier/mL. The particles were also applied with or without a lipid bilayer of DOTAP/DOPC (DD, see Figure 6 a,b).

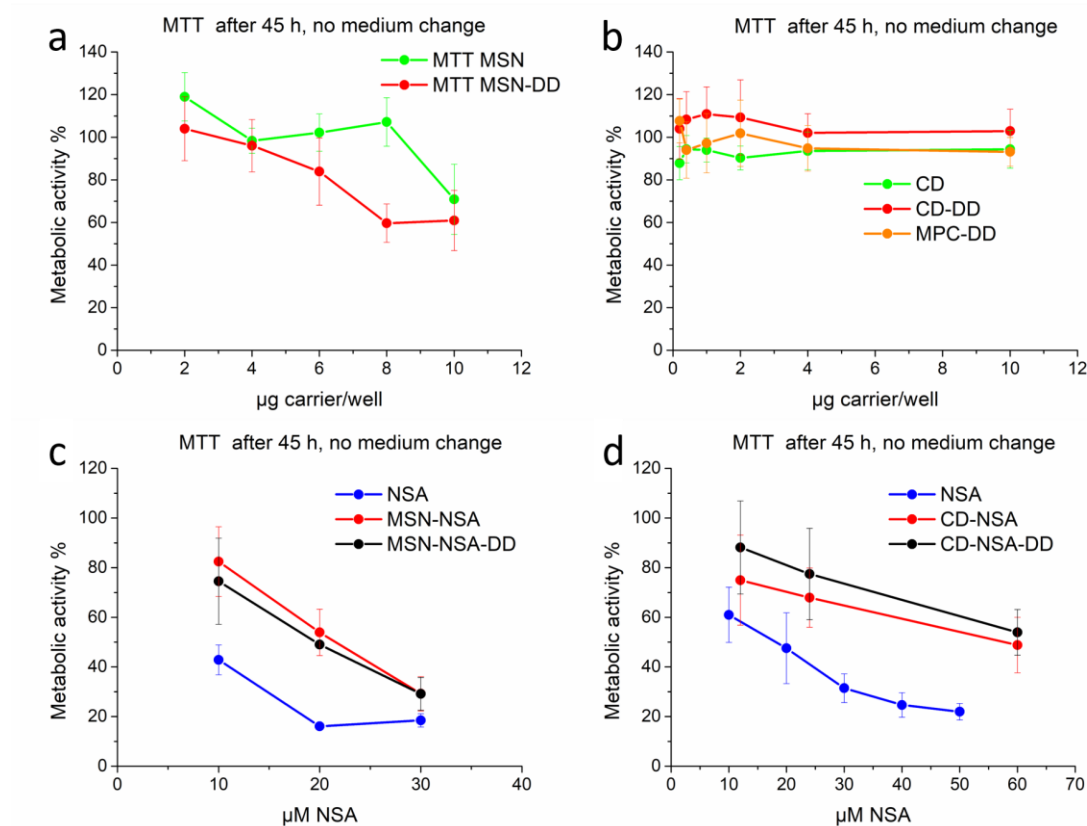


Fig. 6: Assessment of RAW 264.7 cell survival after long incubation times of 45 h without medium change with unloaded and NSA-loaded NP in comparison to exposure to free NSA. a,b) MTT assay of unloaded MSN, CD and MPC particles with and without a lipid bilayer (DD), c,d) MTT assay of MSN and CD NP loaded with NSA. Results are expressed in % as compared to untreated cells.

We also tested the RAW 264.7 metabolic cell activity under comparable conditions with NSA-loaded carriers. In Figure 6 c,d we compared the impact of NSA-loaded MSN and CD carriers with and without a lipid bilayer to that of the free NSA compound at increasing concentrations. A decrease in cell activity was observed with increasing NSA concentrations for both particles. However, cell metabolism was less inhibited by particle-delivered NSA than by the same amount of free NSA. This decreased cell activity was not associated with increased cell death, as observed by live microscopy (See SI, Fig. S11).

In contrast, NSA-loaded MPC-NP completely blocked metabolic activity in RAW 264.7 macrophages already at low NSA concentrations under these conditions. Loading of these MPC particles with NSA required the addition of small concentrations of the surfactant cetyltrimethylammonium chloride (CTAC), which may be detrimental for RAW 264.7 cell survival (see SI, Fig. S10).

We also examined NSA delivery under the more realistic condition of a shorter exposure time as likely encountered in *in vivo* situations and performed a medium exchange after 3 h, while the

final assay was again performed after 45 h. Under these less severe exposure conditions, we did not observe any influence on metabolic cell activity with either MSN-NSA NP or free NSA (see SI, Fig. S12).

### **Porous nanoparticles are taken up by primary macrophages and are not toxic**

Having established that NP delivery of NSA to a macrophage cell line is successful and better tolerated by the cells than the free compound, we examined whether particles were taken up in primary macrophages. To this end, macrophages were differentiated either from freshly isolated murine bone marrow (bone marrow-derived macrophages, BMDM) or from human monocytes isolated from peripheral blood mononuclear cells (PBMC) of healthy volunteers (human monocyte-derived macrophages, hMDM).

To visualize the uptake of NP in primary macrophages, mouse BMDM were incubated with fluorescently labeled MSN (Fig. 7 a) and CD (Fig. 7 b) particles (green) and examined by confocal microscopy. Cellular and endosomal membranes were stained with a lipophilic dye (red). Pictures were taken approximately one minute after particles were added to the cell cultures. Co-localization of the membrane marker and NP signals demonstrated that the NP were rapidly internalized by the macrophages.

To determine whether the porous nanoparticles are toxic in primary macrophages, mouse BMDM and human hMDM were exposed to the NP for 2 hours. The 2-hour time point was chosen because NP release their cargo within 2 hours (see Fig. 4 and Fig. S7, SI). The amount of NP was equal to the maximum concentration used for the functional studies described below. Metabolic activity was assessed by a cell counting kit-8 (CCK-8) assay. This assay, similar to MTT assays, is based on the reduction of a tetrazolium salt in the presence of an electron carrier. A lactate dehydrogenase (LDH) release assay was performed to determine membrane integrity. The assays showed that neither the unloaded particles nor the free NSA at 100  $\mu$ M had an effect on metabolic activity (Fig. 7 c,e) or membrane integrity (Fig. 7 d,f) in mouse BMDM or hMDM after this exposure time.

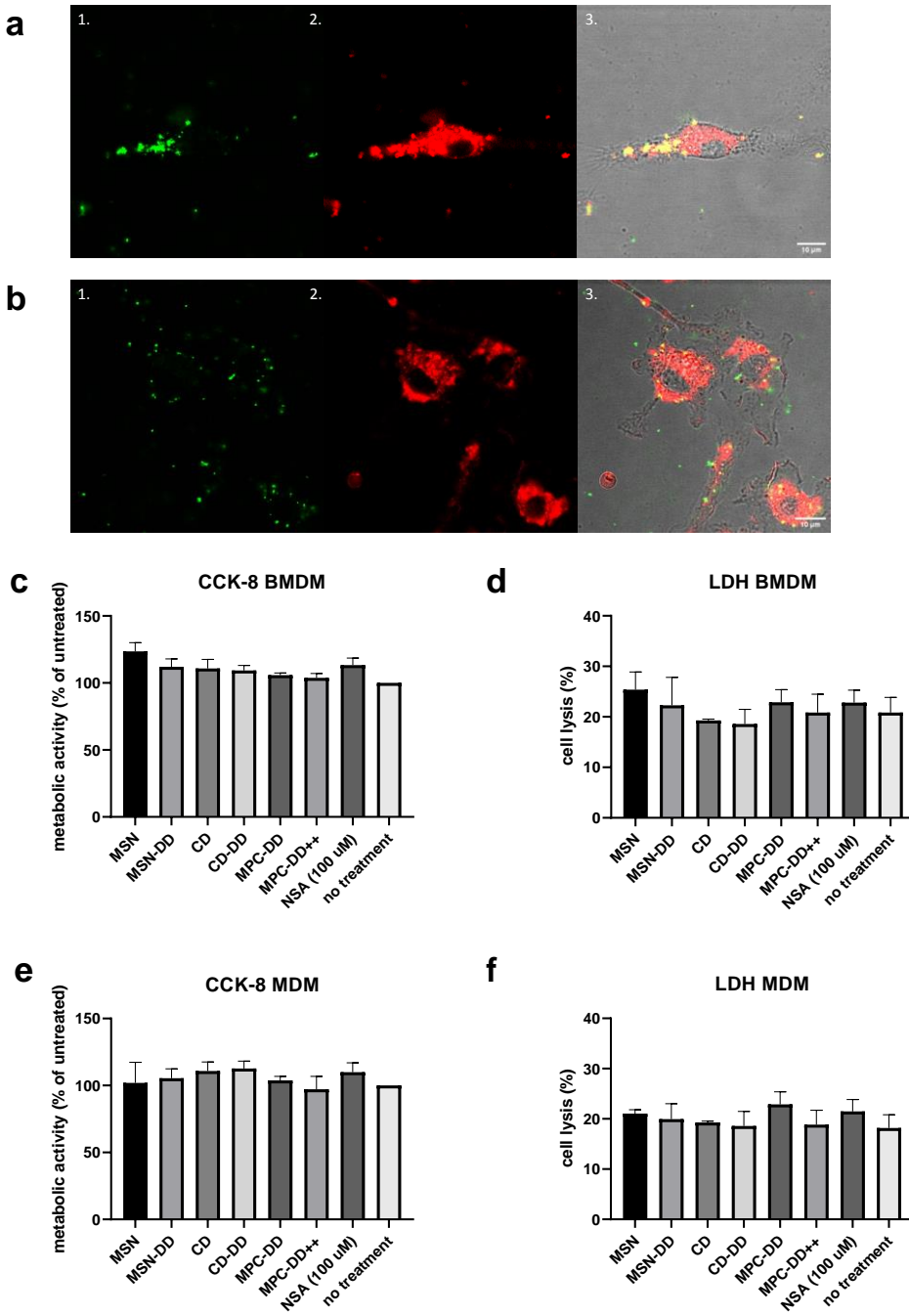


Fig. 7: BMDM were exposed to fluorescently labeled MSN (a) or CD particles (b) for approximately 1 minute. Left) endosomal staining (red), middle) Atto-488 labeled particles (green) and right) merge (red and green), overlay with phase contrast image.

Murine BMDM and human MDM were treated with unloaded NP with and without lipid bilayer (DD) or with free NSA (100 μM). After 2 hours CCK-8 (c,e) and LDH assays (d,f) were performed. (c,e) Metabolic activity of untreated cells was set at 100%. (d,f): LDH release by detergent-lysed control cells was set at 100%.

## NSA prevents IL-1 $\beta$ and IL-18 release from primary macrophages upon GSDMD activation

In a next step, we examined whether we could successfully inhibit GSDMD-mediated cytokine release using NSA. Traditionally, a two-signal model is proposed for the stimulation of GSDMD mediated IL-1 $\beta$  release by immune cells. A first priming signal, such as lipopolysaccharide (LPS), which activates Toll like receptor 4 (TLR4), triggers the intracellular accumulation of pro-IL-1 $\beta$ . Then, a second signal, such as high concentrations of extracellular ATP, leads to activation of caspase 1 and allows for maturation and release of IL-1 $\beta$  through GSDMD pores.[37] Mouse BMDM were primed for 4 hours with LPS, of which the last 30 min included exposure to NSA. After priming, GSDMD was activated by treating the BMDM for 1 hour with ATP (see also scheme in Fig. 9a). Inhibition of GSDMD pore formation was evaluated by measuring secretion of IL-1 $\beta$  and IL-18 into the cell medium by ELISA. LPS combined with ATP induced IL-1 $\beta$  and IL-18 secretion, while LPS or ATP alone did not have an effect on the release of IL-1 $\beta$  or IL-18. NSA dose-dependently inhibited the release of IL-1 $\beta$  and IL-18 induced by the combination of LPS and ATP. At 40  $\mu$ M, NSA was able to completely prevent both IL-1 $\beta$  and IL-18 release from LPS and ATP-treated BMDM (Figure 8 a,b). Because IL-1 $\beta$  and IL-18 release both appear to reflect GSDMD pore formation equally well, we decided to continue using IL-1 $\beta$  release as a readout for GSDMD activation.

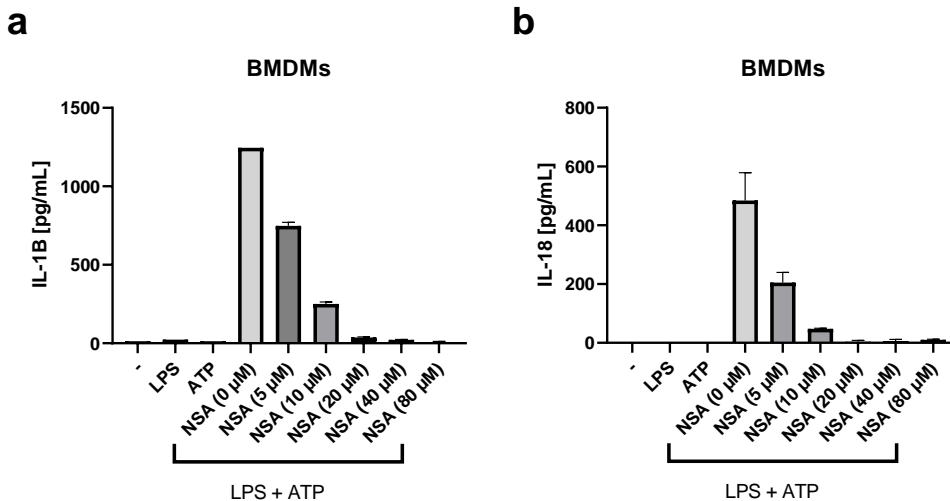


Fig. 8: Concentration of a) IL-1 $\beta$  and b) IL-18 in cell culture supernatant after mouse BMDM were treated with LPS (100 ng/ml), ATP (5 mM) and NSA at increasing concentrations.



### **NSA-loaded nanoparticles inhibit IL-1 $\beta$ release from murine BMDM and human MDM in a dose-dependent manner**

Next, we investigated whether porous NP could successfully deliver NSA to BMDM and inhibit the release of IL-1 $\beta$ . As in Figure 8, the LPS and ATP combination was used to activate GSDMD in BMDM. NSA-loaded NPs were added to BMDM during the last 2 hours of priming with LPS (see priming/activation scheme in Figure 9a). After priming, the cell culture medium was exchanged to remove LPS and cells were activated with ATP for 1 hour. Cells were exposed to NP containing NSA concentrations of up to 60  $\mu$ M, considering that particle-delivered NSA concentrations of up to 80  $\mu$ M were well tolerated in RAW 264.7 cells (see SI, Fig. S13), and that IL-1 $\beta$  release was completely inhibited in BMDM at 40  $\mu$ M of free NSA (see figure 8a). ELISA assays were performed to measure IL-1 $\beta$  release and values were expressed as % of response to unloaded particles, to allow for comparison with other cells types described below. All NSA-loaded particles inhibited GSDMD-mediated IL-1 $\beta$  release in a dose-dependent manner (Fig. 9b-g). However, only CD particles were able to fully prevent the release of IL-1 $\beta$ , similar to the effect of free NSA (Fig. 9d).

Empty MSN, MSN-DD and CD particles did not induce release of IL-1 $\beta$  from unstimulated mouse BMDM, nor by human MDM (See SI, S14a and b). Only the empty MPC-DD++ and CD-DD particles induced small amounts of IL-1 $\beta$  release, suggesting that these particles may cause low levels of inflammation. Empty MSN, CD and MPC particles with and without lipid bilayers did not inhibit LPS+ATP-induced IL-1 $\beta$  release (See SI, S14c and d).

To determine if the IL-1 $\beta$  suppression with NSA-loaded nanoparticles seen in primary murine macrophages could also be observed in human macrophages, hMDM were activated with the LPS+ATP combination and exposed to NP according to the activation scheme in figure 9a. In human macrophages, all NSA-loaded particles showed a dose-dependent inhibitory effect on IL-1 $\beta$  release. As seen with BMDM, the strongest inhibition was observed with NSA-loaded CD particles (Fig. 10 a-f). Thus, porous NP can successfully deliver NSA to both mouse and human macrophages, allowing a strong inhibition of IL-1 $\beta$  release in the absence of particle toxicity.

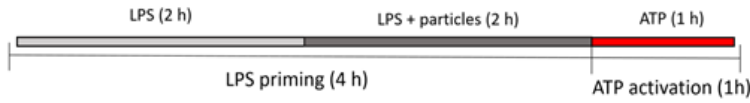
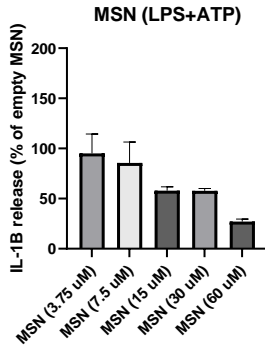
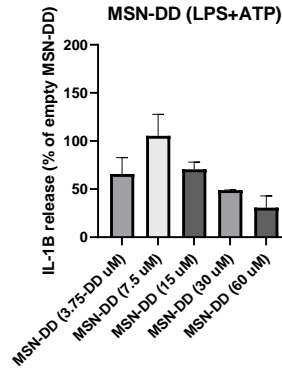
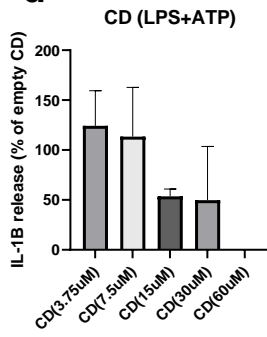
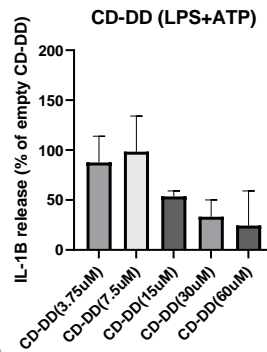
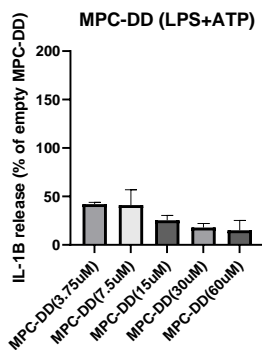
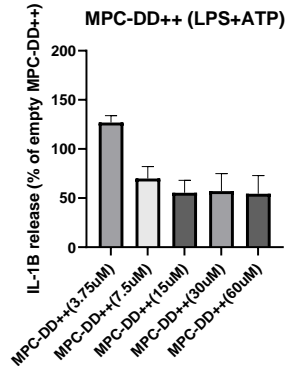
**a****b****c****d****e****f****g**

Fig. 9: IL-1 $\beta$  release by mouse BMDM exposed to NSA-loaded nanoparticles: a) cells were primed for 2 hours with LPS and 2 hours additionally with particles. After 4 hours of priming, cells were treated with ATP to activate caspase 1 and GSDMD.

b) MSN, b) MSN-DD, c) CD, d) CD-DD, e) MPC-DD, f) MPC-DD++. Particles were used empty and NSA-loaded, containing NSA at final well concentrations of 3.75, 7.5, 15, 30, and 60  $\mu\text{M}$ .

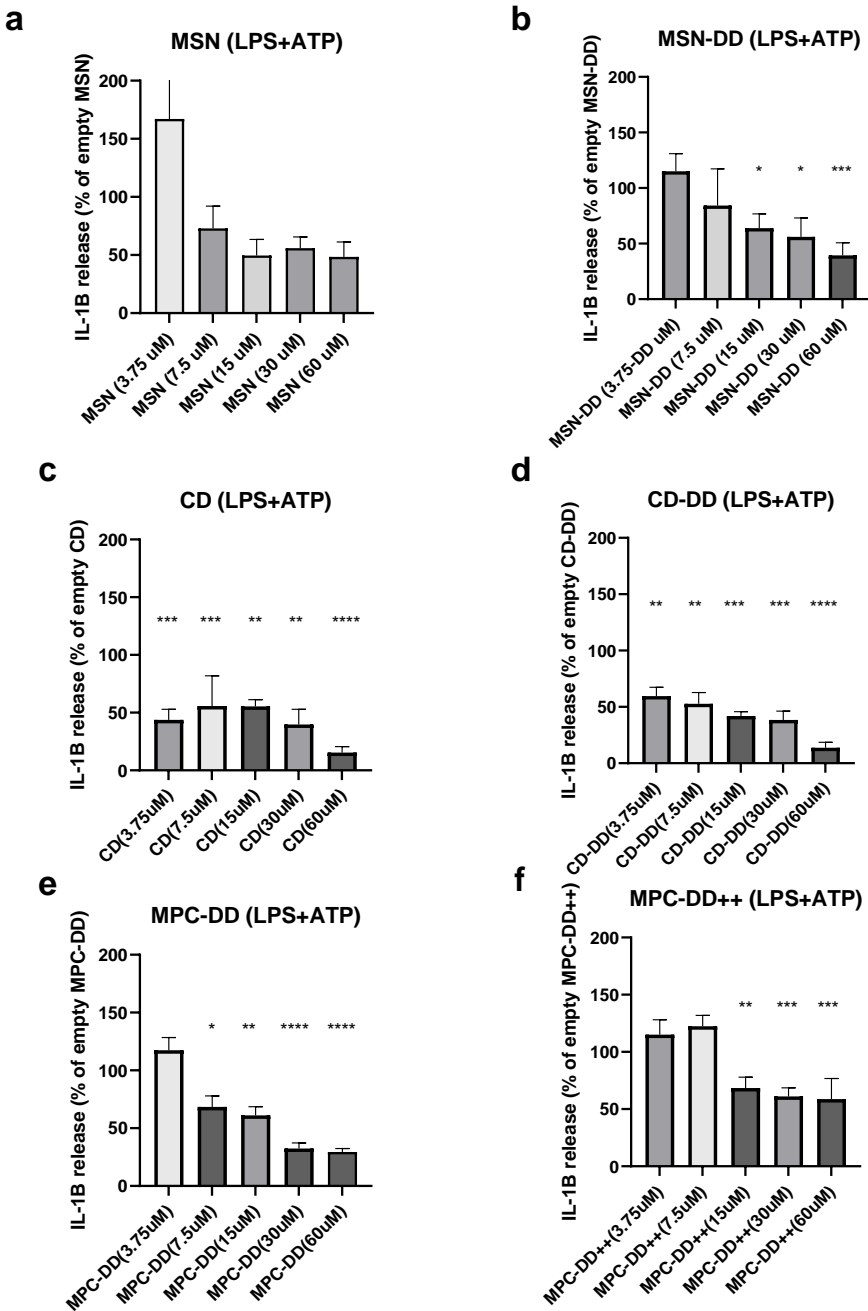


Fig. 10: IL-1 $\beta$  release by human MDM: cells were activated with LPS and ATP as in Figure 9. a) MSN, b) MSN-DD, c) CD, d) CD-DD, e) MPC-DD, f) MPC-DD++. Particles were used empty and containing NSA at final well concentrations of 3.75, 7.5, 15, 30, and 60  $\mu\text{M}$ .

## Nanoparticles are preferentially taken up by phagocytes such as macrophages

Since myeloid cells, such as macrophages, are the main producers of the proinflammatory cytokines IL-1 $\beta$  and IL-18 in a GSDMD-dependent manner, it is of great interest to target NSA specifically to these cell types in order to avoid off-target effects of the drug. NP provide an opportunity to selectively deliver the drug to these cells, as myeloid cells are professional phagocytes and are well-known to take up particulate material.[25]

To determine whether the NP in this work permit effective targeting of myeloid cells, murine splenocytes were exposed to the different types of porous particles. Mouse splenocytes are composed of different immune cell populations, including myeloid cells, such as macrophages and dendritic cells, as well as B and T lymphocytes.[38] Freshly isolated splenocytes were cultured with fluorescently-labeled MSN, MSN-DD, CD and CD-DD particles for 2, 6 and 24 hours. An acidic wash (pH 3) was performed to remove surface-bound particles as previously described.[39] Immune cell types, their viability and their positivity for the fluorescent NP were determined by flow cytometry (see SI, Fig. S15 for gating strategy used). Viability was assessed for the CD45.2-positive cells, representing all immune cells within the splenocytes. No decrease in viability was observed at any of the timepoints, after exposure to the different porous NP compared to untreated cells (Figure 11a).

The percentage of NP-positive cells was measured for dendritic cells, macrophages, B cells and T cells. After 2 hours, the proportion of positive cells within each cell type ranged from 5% to 30% and was similar among the different cell types (Fig. 11 b). Overall, particles with a lipid bilayer tended to be taken up less than their non-coated counterparts. **This effect may be traced to a bilayer-induced modulation of the metabolism in the phagocytic cells.**[40] After 24 hours, over 70% of dendritic cells and over 40% of macrophages and B cells were positive for uncoated CD particles, whereas less than 20% of T cells were positive for these particles. Less than 10% of all cell types were positive for MSN and MSN-DD. Thus, CD particles were taken up by a high proportion of phagocytic cells including dendritic cells, macrophages and B cells, but much less by T cells, which are non-phagocytic cells.

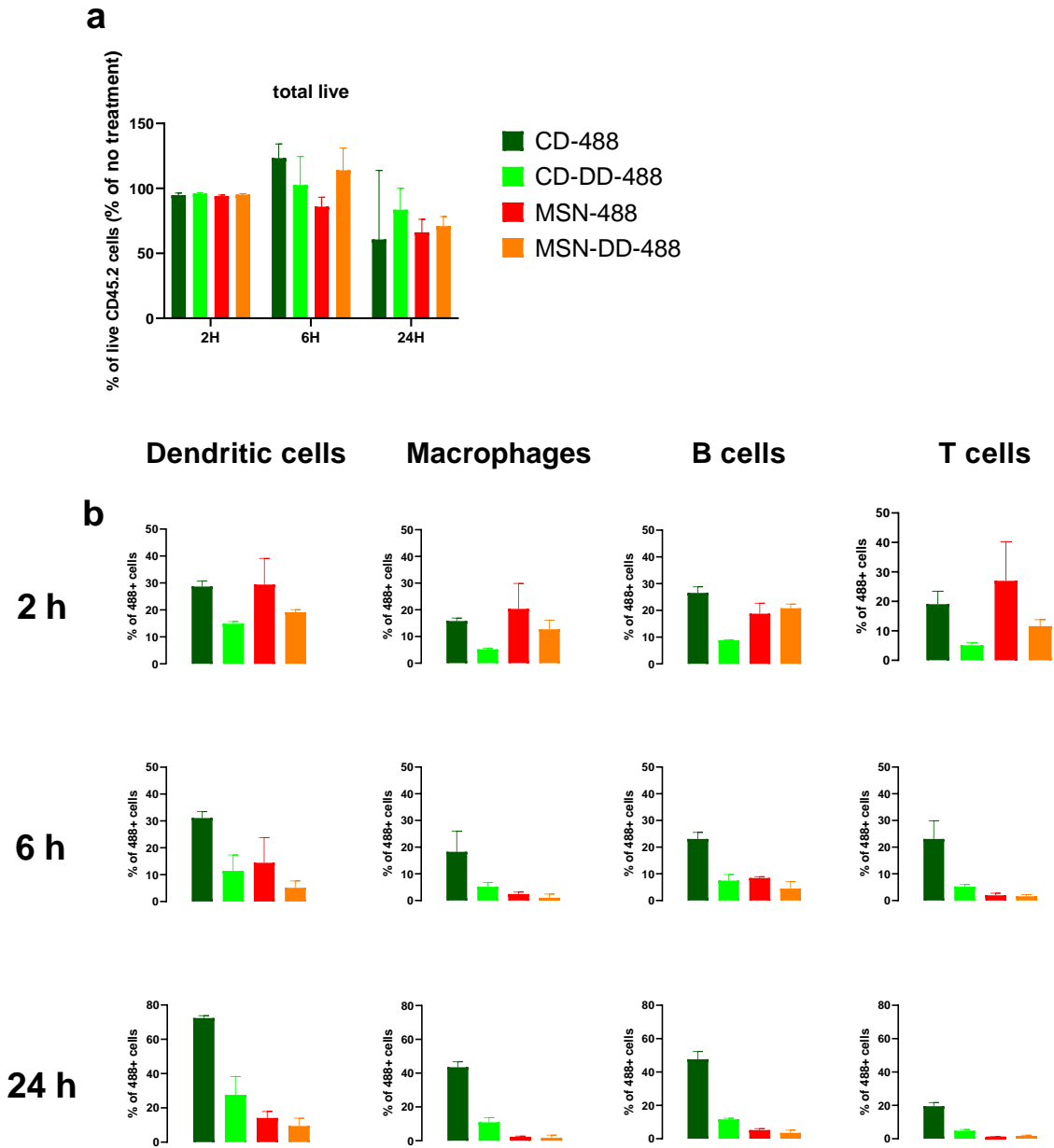


Fig. 11: a) Percentage of live CD45.2+ splenocytes after treatment with CD (dark green), CD-DD (light green), MSN (red) and MSN-DD (orange) particles compared to untreated cells after 2 h, 6 h and 24 h. b) Percentage of NP-positive dendritic cells (CD11c+), macrophages (CD11b+, CD11c-), B cells (CD19+) and T cells (CD3+) after 2 h, 6 h and 24 h.

## Discussion

NSA was recently discovered as a specific antagonist against GSDMD-mediated pyroptotic cell death and inflammatory cytokine release. One of the major cell types that express GSDMD are macrophages, which play an important role for the initiation of inflammatory processes. It is therefore relevant to target NSA specifically to these cells in order to limit inflammation, while at the same time preventing unwanted toxicity of the drug to other cell types.[8] The use of NP as delivery system can allow for the selective targeting of macrophages, since these cells are specialized in the uptake of particulate material.[25] We could show that the highly hydrophobic NSA can be absorbed into three different nanocarriers at high loading, allowing for a solvent-free delivery of NSA. Both MSN and CD particles were rapidly taken up by macrophages and delivered their NSA cargo into the cells. After 24h of exposure to a mixed population of immune cells, a high proportion of macrophages and dendritic cells, which are also phagocytic cells with inflammatory properties, were positive for CD particles. Interestingly, a substantial percentage of B lymphocytes was also positive for CD particles after 24h. B lymphocytes are capable of phagocytosis,[41] and we have previously shown that B lymphocytes can take up certain types of particles such as gold nanoparticles.[42] In contrast, few T cells, which are non-phagocytic cells, were positive for CD particles. This suggests that NSA delivery by porous NP may be an effective manner to target macrophages and dendritic cells as the main initiators of inflammation.

Utilizing a macrophage cell line, as well as freshly differentiated primary macrophages from mice and human donors in a variety of in vitro studies, we showed a good compatibility of all unloaded carriers with these cell types, even in long-term incubation experiments of over 45 h. The particles themselves did not induce inflammation in macrophages, with the exception of lipid-coated MPC-DD++ and CD-DD particles. This lipid bilayer coating was applied to evaluate its effect on the speed of cellular uptake as well as a protective coating, preventing premature release of NSA. Since we did not observe major release of NSA even from uncoated NP and did recognize a reduced effect of DD-covered NP with respect to IL-1 $\beta$  suppression, we conclude that for future applications bilayer-free particles can be used advantageously, thus avoiding potential immune responses.

We have previously shown that different types of NP can be taken up into phagocytic cells without immune activation.[43] In contrast, other particles, including certain types of silica-based NP, can induce inflammation and GSDMD-mediated pyroptosis in macrophages.[44, 45] Early screening for proinflammatory effects in standardized conditions is therefore essential during the development of particles for clinical applications.[25]

When loaded with NSA, MSN and CD NP were better tolerated by macrophages than the free NSA compound, which forms aggregates in aqueous media. In contrast, NSA-loaded MPC particles completely blocked metabolic activity of macrophages even at low NSA concentrations. MPC particles require small amounts of surfactant for loading of NSA, which may have toxic

effects on these cells.[46] Thus, with the exception of MPC particles, delivery by porous NP may enhance the compatibility of NSA with macrophages.

In functional assays with freshly differentiated macrophages from mice and human donors, a concentration-dependent suppression of IL-1 $\beta$  release was established with all three types of NP. The strongest suppressive effect on human macrophages was obtained with CD particles and was observed already at the lowest NSA concentrations. None of the unloaded particles impaired IL-1 $\beta$  release after GSDMD activation, demonstrating that the anti-inflammatory effect is due to the drug cargo rather than to the carrier.

In summary, our screening of particles has established two valuable candidates for NSA delivery in the form of MSN and CD-CDI NP. Both particles are easily synthesized, scalable, storable as well as biodegradable and can deliver high contents of this hydrophobic molecule without further application of a capping layer to phagocytic cells, inducing a successful suppression of the IL-1 $\beta$  cytokine. While MSN NP are rapidly taken up in large numbers by macrophages, we established that CD-NP are apparently even more effective in intracellular NSA release, leading to the highest reduction of the IL-1 $\beta$  cytokine.

Here, we have focused on the characterization of different NSA-NP systems and on their *in vitro* effects on macrophages and other immune cells. However, we expect additional benefits of these nanoparticle formulations *in vivo*. Indeed, we have previously shown that following subcutaneous injection, MSN nanoparticles accumulate in phagocytic cells in the lymph nodes draining the injection site.[19] Nanoparticle formulation may therefore also allow for site-specific, DMSO-free delivery of NSA *in vivo*.

This study establishes the potential of porous biocompatible NP for the effective and targeted delivery of potentially toxic, hydrophobic drugs in order to regulate inflammatory responses in both primary murine and human immune cells.

## Acknowledgements

The authors thank the Deutsche Forschungsgemeinschaft (DFG) for financial support (SFB 1032). Additional support is gratefully acknowledged from the Excellence Cluster Nanosystems Initiative Munich (NIM) and from the Center for NanoScience Munich (CeNS). We thank the Swiss National Science Foundation (grant 182317 to CB and 188470 to GP) for financial support. We thank the research group of Prof. E. Wagner, Department of Pharmacy at the LMU Munich for sharing their RAW 264.7 cells. The authors would like to acknowledge Montserrat Alvarez for her technical support. Scheme 1 was designed using Biorender.

## References

- [1] M.G. Netea, F. Balkwill, M. Chonchol, F. Cominelli, M.Y. Donath, E.J. Giamarellos-Bourboulis, D. Golenbock, M.S. Gresnigt, M.T. Heneka, H.M. Hoffman, R. Hotchkiss, L.A.B. Joosten, D.L. Kastner, M. Korte, E. Latz, P. Libby, T. Mandrup-Poulsen, A. Mantovani, K.H.G. Mills, K.L. Nowak, L.A. O'Neill, P. Pickkers, T. van der Poll, P.M. Ridker, J. Schalkwijk, D.A. Schwartz, B. Siegmund, C.J. Steer, H. Tilg, J.W.M. van der Meer, F.L. van de Veerdonk, C.A. Dinarello, A guiding map for inflammation, *Nature Immunology*, 18 (2017) 826-831.
- [2] D. Zamarin, B. Holmgaard Rikke, K. Subudhi Sumit, S. Park Joon, M. Mansour, P. Palese, T. Merghoub, D. Wolchok Jedd, P. Allison James, Localized Oncolytic Virotherapy Overcomes Systemic Tumor Resistance to Immune Checkpoint Blockade Immunotherapy, *Science Translational Medicine*, 6 (2014) 226ra232-226ra232.
- [3] B. Boersma, W. Jiskoot, P. Lowe, C. Bourquin, The interleukin-1 cytokine family members: Role in cancer pathogenesis and potential therapeutic applications in cancer immunotherapy, *CYTOKINE & GROWTH FACTOR REVIEWS*, 62 (2021) 1-14.
- [4] W.-t. He, H. Wan, L. Hu, P. Chen, X. Wang, Z. Huang, Z.-H. Yang, C.-Q. Zhong, J. Han, Gasdermin D is an executor of pyroptosis and required for interleukin-1 $\beta$  secretion, *Cell Research*, 25 (2015) 1285-1298.
- [5] J. Shi, Y. Zhao, K. Wang, X. Shi, Y. Wang, H. Huang, Y. Zhuang, T. Cai, F. Wang, F. Shao, Cleavage of GSDMD by inflammatory caspases determines pyroptotic cell death, *Nature*, 526 (2015) 660-665.
- [6] J. Ding, K. Wang, W. Liu, Y. She, Q. Sun, J. Shi, H. Sun, D.-C. Wang, F. Shao, Pore-forming activity and structural autoinhibition of the gasdermin family, *Nature*, 535 (2016) 111-116.
- [7] J. Ruan, S. Xia, X. Liu, J. Lieberman, H. Wu, Cryo-EM structure of the gasdermin A3 membrane pore, *Nature*, 557 (2018) 62-67.
- [8] X. Chen, W.-t. He, L. Hu, J. Li, Y. Fang, X. Wang, X. Xu, Z. Wang, K. Huang, J. Han, Pyroptosis is driven by non-selective gasdermin-D pore and its morphology is different from MLKL channel-mediated necroptosis, *Cell Research*, 26 (2016) 1007-1020.
- [9] J.J. Hu, X. Liu, S. Xia, Z. Zhang, Y. Zhang, J. Zhao, J. Ruan, X. Luo, X. Lou, Y. Bai, J. Wang, L.R. Hollingsworth, V.G. Magupalli, L. Zhao, H.R. Luo, J. Kim, J. Lieberman, H. Wu, FDA-approved disulfiram inhibits pyroptosis by blocking gasdermin D pore formation, *Nature Immunology*, 21 (2020) 736-745.
- [10] K. Rathkey Joseph, J. Zhao, Z. Liu, Y. Chen, J. Yang, C. Kondolf Hannah, L. Benson Bryan, M. Chirieleison Steven, Y. Huang Alex, R. Dubyak George, S. Xiao Tsan, X. Li, W. Abbott Derek, Chemical disruption of the pyroptotic pore-forming protein gasdermin D inhibits inflammatory cell death and sepsis, *Science Immunology*, 3 (2018) eaat2738.
- [11] Y. Bai, H.C. Lam, X. Lei, Dissecting Programmed Cell Death with Small Molecules, *Acc. Chem. Res.*, 53 (2020) 1034-1045.
- [12] S. Chen, W. Lai, X. Li, H. Wang, Necrosulfonamide Selectively Induces DNA Double-Strand Breaks in Acute Myeloid Leukemia Cells, *Chemical Research in Toxicology*, 35 (2022) 387-391.
- [13] M.J. Mitchell, M.M. Billingsley, R.M. Haley, M.E. Wechsler, N.A. Peppas, R. Langer, Engineering precision nanoparticles for drug delivery, *Nature Reviews Drug Discovery*, 20 (2021) 101-124.
- [14] V. Mamaeva, C. Sahlgren, M. Linden, Mesoporous silica nanoparticles in medicine-Recent advances, *Adv. Drug Delivery Rev.*, 65 (2013) 689-702.
- [15] Y. Li, X. Zhang, X. Liu, W. Pan, N. Li, B. Tang, Designing and Engineering of Nanocarriers for Bioapplication in Cancer Immunotherapy, *ACS Applied Bio Materials*, (2020).
- [16] Y. Gao, D. Gao, J. Shen, Q. Wang, A Review of Mesoporous Silica Nanoparticle Delivery Systems in Chemo-Based Combination Cancer Therapies, *Frontiers in Chemistry*, 8 (2020) 1086.



- [17] A. Carvalho, R. Cordeiro, H. Faneca, Silica-Based Gene Delivery Systems: From Design to Therapeutic Applications, *Pharmaceutics*, 12 (2020) 649.
- [18] J.J. Aguilera-Correa, J. Esteban, M. Vallet-Regí, Inorganic and Polymeric Nanoparticles for Human Viral and Bacterial Infections Prevention and Treatment, *Nanomaterials*, 11 (2021).
- [19] J. Wagner, D. Gößl, N. Ustyanovska, M. Xiong, D. Hauser, O. Zhuzhgova, S. Hočevár, B. Taskoparan, L. Poller, S. Datz, H. Engelke, Y. Daali, T. Bein, C. Bourquin, Mesoporous Silica Nanoparticles as pH-Responsive Carrier for the Immune-Activating Drug Resiquimod Enhance the Local Immune Response in Mice, *ACS Nano*, 15 (2021) 4450-4466.
- [20] S. Heidegger, D. Gößl, A. Schmidt, S. Niedermayer, C. Argyo, S. Endres, T. Bein, C. Bourquin, Immune response to functionalized mesoporous silica nanoparticles for targeted drug delivery, *Nanoscale*, 8 (2016) 938-948.
- [21] R. Challa, A. Ahuja, J. Ali, R.K. Khar, Cyclodextrins in drug delivery: An updated review, *AAPS PharmSciTech*, 6 (2005) E329-E357.
- [22] G. Tejashri, B. Amrita, J. Darshana, Cyclodextrin based nanosponges for pharmaceutical use: A review, *Acta Pharmaceutica*, 63 (2013) 335-358.
- [23] J.R. Lakkakula, R.W.M. Krause, A vision for cyclodextrin nanoparticles in drug delivery systems and pharmaceutical applications, *Nanomedicine*, 9 (2014) 877-894.
- [24] R. Cavalli, F. Trotta, W. Tumiatti, Cyclodextrin-based Nanosponges for Drug Delivery, *Journal of inclusion phenomena and macrocyclic chemistry*, 56 (2006) 209-213.
- [25] I. Mottas, A. Milosevic, A. Petri-Fink, B. Rothen-Rutishauser, C. Bourquin, A rapid screening method to evaluate the impact of nanoparticles on macrophages, *Nanoscale*, 9 (2017) 2492-2504.
- [26] L. Wehl, C. von Schirnding, M.C. Bayer, O. Zhuzhgova, H. Engelke, T. Bein, Mesoporous Biodegradable Magnesium Phosphate-Citrate Nanocarriers Amplify Methotrexate Anticancer Activity in HeLa Cells, *Bioconjugate Chemistry*, (2022).
- [27] J.G. Croissant, Y. Fatieiev, N.M. Khashab, Degradability and Clearance of Silicon, Organosilica, Silsesquioxane, Silica Mixed Oxide, and Mesoporous Silica Nanoparticles, *Adv. Mater.*, 29 (2017) 1604634.
- [28] K. Möller, T. Bein, Degradable Drug Carriers: Vanishing Mesoporous Silica Nanoparticles, *Chemistry of Materials*, 31 (2019) 4364-4378.
- [29] C. Argyo, V. Weiss, C. Bräuchle, T. Bein, Multifunctional Mesoporous Silica Nanoparticles as a Universal Platform for Drug Delivery, *Chem. Mater.*, 26 (2014) 435-451.
- [30] K. Möller, T. Bein, Talented Mesoporous Silica Nanoparticles, *Chem. Mater.*, 29 (2017) 371-388.
- [31] S. Lucia Appleton, S. Navarro-Orcajada, F.J. Martínez-Navarro, F. Caldera, J.M. López-Nicolás, F. Trotta, A. Matencio, Cyclodextrins as Anti-inflammatory Agents: Basis, Drugs and Perspectives, *Biomolecules*, 11 (2021).
- [32] F. Trotta, R. Cavalli, Characterization and Applications of New Hyper-Cross-Linked Cyclodextrins, *Composite Interfaces*, 16 (2009) 39-48.
- [33] I. Krabicová, S.L. Appleton, M. Tannous, G. Hoti, F. Caldera, A. Rubin Pedrazzo, C. Ceccone, R. Cavalli, F. Trotta, History of Cyclodextrin Nanosponges, *Polymers*, 12 (2020).
- [34] S. Datz, B. Illes, D. Gößl, C.v. Schirnding, H. Engelke, T. Bein, Biocompatible crosslinked  $\beta$ -cyclodextrin nanoparticles as multifunctional carriers for cellular delivery, *Nanoscale*, 10 (2018) 16284-16292.
- [35] K. Möller, B. Macaulay, T. Bein, Curcumin Encapsulated in Crosslinked Cyclodextrin Nanoparticles Enables Immediate Inhibition of Cell Growth and Efficient Killing of Cancer Cells, *Nanomaterials*, 11 (2021).
- [36] L. Wehl, C. von Schirnding, M.C. Bayer, O. Zhuzhgova, H. Engelke, T. Bein, Mesoporous Biodegradable Magnesium Phosphate-Citrate Nanocarriers Amplify Methotrexate Anticancer Activity in HeLa Cells, *Bioconjugate Chemistry*, 33 (2022) 566-575.

- [37] Y. Yang, H. Wang, M. Kouadir, H. Song, F. Shi, Recent advances in the mechanisms of NLRP3 inflammasome activation and its inhibitors, *Cell Death & Disease*, 10 (2019) 128.
- [38] V.J. Schüller, S. Heidegger, N. Sandholzer, P.C. Nickels, N.A. Suhartha, S. Endres, C. Bourquin, T. Liedl, Cellular Immunostimulation by CpG-Sequence-Coated DNA Origami Structures, *ACS Nano*, 5 (2011) 9696-9702.
- [39] I. Mellman, H. Plutner, P. Ukkonen, Internalization and rapid recycling of macrophage Fc receptors tagged with monovalent antireceptor antibody: possible role of a prelysosomal compartment, *Journal of Cell Biology*, 98 (1984) 1163-1169.
- [40] A.K. Dey, A. Nougarede, F. Clément, C. Fournier, E. Jouvin-Marche, M. Escudé, D. Jary, F.P. Navarro, P.N. Marche, Tuning the Immunostimulation Properties of Cationic Lipid Nanocarriers for Nucleic Acid Delivery, *Frontiers in Immunology*, 12 (2021), Article 722411.
- [41] A. Martínez-Riaño, E.R. Bovolenta, P. Mendoza, C.L. Oeste, M.J. Martín-Bermejo, P. Bovolenta, M. Turner, N. Martínez-Martín, B. Alarcón, Antigen phagocytosis by B cells is required for a potent humoral response, *EMBO reports*, 19 (2018) e46016.
- [42] S. Hočevár, A. Milošević, L. Rodriguez-Lorenzo, L. Ackermann-Hirschi, I. Mottas, A. Petri-Fink, B. Rothen-Rutishauser, C. Bourquin, M.J.D. Clift, Polymer-Coated Gold Nanospheres Do Not Impair the Innate Immune Function of Human B Lymphocytes in Vitro, *ACS Nano*, 13 (2019) 6790-6800.
- [43] N. Héroult, J. Wagner, S. Abram, J. Widmer, J. Horvath, D. Vanhecke, C. Bourquin, K. Fromm, Silver-Containing Titanium Dioxide Nanocapsules for Combating Multidrug-Resistant Bacteria, *Int J Nanomedicine*, 15 (2020) 1267-1281.
- [44] H. Yin, L. Fang, L. Wang, Y. Xia, J. Tian, L. Ma, J. Zhang, N. Li, W. Li, S. Yao, L. Zhang, Acute Silica Exposure Triggers Pulmonary Inflammation Through Macrophage Pyroptosis: An Experimental Simulation, *Frontiers in Immunology*, 13 (2022).
- [45] M. Tsugita, N. Morimoto, M. Nakayama, SiO<sub>2</sub> and TiO<sub>2</sub> nanoparticles synergistically trigger macrophage inflammatory responses, *Particle and fibre toxicology*, 14 (2017) 1-9.
- [46] H. Li, X. Tao, E. Song, Y. Song, Iron oxide nanoparticles oxidize transformed RAW 264.7 macrophages into foam cells: Impact of pulmonary surfactant component dipalmitoylphosphatidylcholine, *Chemosphere*, 300 (2022) 134617.



Click here to access/download

**Supplementary Material**

Supplemental Information Manuscript COREL-D-22-  
01606.docx



## Author credit statement

All persons who meet authorship criteria are listed as authors, and all authors certify that they have participated sufficiently in the work to take public responsibility for the content, including participation in the concept, design, analysis, writing, or revision of the manuscript.